

Simple and fast process using hydrochloric acid for producing synthetic zinc-rich stevensite

T. C. Carvalho^{1*}, B. B. Michel¹, M. G. Silva-Valenzuela¹, E. Hildebrando²,
R. F. Neves², F. R. Valenzuela-Diaz¹

¹University of S. Paulo, Polytechnic School, Applied Clays Laboratory, S. Paulo, SP, Brazil

²Federal University of Pará, Belém, PA, Brazil

Abstract

In the last decades, clays have been used in sectors such as health and cosmetics. This requires products that are increasingly pure and present homogeneous properties, hardly found in natural clays. The use of synthetic clays can be a solution. For this, it is necessary to explore techniques for their production. The main focus of this study was to synthesize a smectite clay in a simple, fast and economic way at low temperature and pressure, called static and dynamic methods. To regulate the pH of the reaction and bring it closer to the ideal synthesis conditions, two different acids were used: nitric acid (the most widely used in the literature) and hydrochloric acid (more accessible and cheaper). The results showed characteristics of uniform crystalline material with a porous structure similar to that of the smectite group. Small particle sizes of approximately 100 nm were observed by scanning electron microscopy. Stevensite clay was obtained by both synthesis methods using two different acids; the static method with hydrochloric acid stood out. The greater practicality in its development provides a more viable option for large-scale industrial production.

Keywords: synthetic clay minerals, stevensite, ceramic properties.


INTRODUCTION

Smectite clays belong to the 2:1 phyllosilicate group and are important materials for a wide variety of applications, such as ceramics, rheological additives, binders, sorbents, ion exchangers, and molecular sieve catalysts [1, 2]. The variety of its applications derives from its chemical and physical properties, such as high cation exchange capacity (CEC) and high surface area [3]. The vast majority of works that use clay as a raw material use natural clays [4] due to their good properties, low cost, and easy access. However, clay minerals in their natural forms have diverse mineralogical compositions and are associated with several metallic ions and contaminants that negatively influence thermo-oxidative stability [5, 6]. According to Pascua et al. [7], the removal of crystalline impurities is difficult, and currently applied processing procedures can irreversibly and unpredictably alter the physicochemical properties of smectites. These negative factors may imply limits on the application of natural material in some industrial and academic processes, increasing the interest in synthetic clay minerals produced in the laboratory, under controlled conditions, and known compositions. Mostly due to the composition and projected structures of these clays, they can provide advanced functional materials for new applications or studies that require homogeneous and well-defined samples [8, 9]. Some

examples are the incomplete exfoliation of polypropylene (PP) nanocomposites related to impurities [10] and the incomplete organophilization of clays [11].

Over the past 60 years, numerous smectite synthesis experiments have been carried out under different conditions of temperature, pressure, and moderate or extreme hydrothermal treatment [12, 13]. The main objective of the procedures is to obtain pure samples in less time and at lower temperatures. These two parameters are important in re-creating the formation of mineral clay on a laboratory scale and in reducing the energy required for clay synthesis [14], as most conditions are high temperature/pressure. Some trioctahedral smectite clay minerals [3], such as saponite, hectorite, and stevensite, can be synthesized at low temperatures and pressures by the hydrolysis of urea; however, they use more sophisticated methods, with the use of reactors, electrolytic buffers, and autotitrator [15, 16], increasing the cost of manufacturing and hindering the industrial use of synthetic clays. Stevensite is trioctahedral smectite, which contains an octahedral sheet rich in divalent cations (Zn^{2+} , Co^{2+} , Mg^{2+} among others) and a tetrahedral sheet rich in Si [17]. It has a basal space of around 13 to 15 Å [15, 18], but natural stevensite clay has impurities such as calcite, dolomite, and quartz that can affect its use in specific applications favoring the use of synthetic clays [19]. The study on the application of this synthetic material has been limited to the use of heterogeneous catalysts for hydrodesulfurization, nanofillers for clay-polymer nanocomposites [12, 15, 20], additives for the pharmaceutical industry [19, 20], and permeable reactive barriers [21]. Sorbents for removing metals from water and

*thamyrescc@usp.br

 <https://orcid.org/0000-0002-9669-0282>

wastewater [22] have also been studied and demonstrated promising expectations.

Most of the literature related to this subject describes long and complex methods with expensive reagents (nitric acid, sulfuric acid) and laboratory instruments (autotitrator, hydrothermal reactor). One of them was performed by Decarreau [23], who developed a method for synthesizing hectorite and stevensite in thermostatic reactors, using sodium silicate, magnesium chloride (or sulfate), and hydrochloric (or sulfuric) acid. To complete the reaction of synthesis, lithium fluoride (or lithium chloride) was added to the hectorite solution and calcium chloride to the stevensite solution. The precursors were dispersed in water at temperatures from 5 to 90 °C for periods of 2 to 3 weeks with magnetic stirring. The formation of synthetic products of stevensite and hectorite equivalent to natural ones was confirmed after the two-week period at 75 °C. Khassin et al. [24] prepared stevensite of zinc (Zn), magnesium (Mg), cobalt (Co), and Co-Zn, and evaluated their structural properties during calcination in different media (air, inert gas flow, and reduction of hydrogen). The syntheses of the clays were produced by the precipitation method, using aerosil silica, cobalt nitrate hexahydrate $[\text{Co}(\text{NO}_3)_2 \cdot 6\text{H}_2\text{O}]$, zinc nitrate hexahydrate $[\text{Zn}(\text{NO}_3)_2 \cdot 6\text{H}_2\text{O}]$, urea and pH set at 3.5. Magnesium samples were synthesized in two steps: first, an aqueous solution of silicon dioxide (SiO_2) and nitric acid (HNO_3), with pH set at 2.3 was heated at 60 °C for a period of 12 h, producing a SiO_2 paste. The second stage included mixing cobalt nitrate hexahydrate with potassium hydroxide (KOH) and sodium carbonate (K_2CO_3) at 65 °C and pH 10.7, added to the SiO_2 paste of the first phase. The final product was heated at 95 °C and agitated for 24 h, then washed and dried under an IR lamp. The precipitation method synthesized a stevensite clay and it was possible to observe a cobalt stevensite in the pH range of 4-10. Further analysis of calcined samples under inert gas or air flow suggested that cobalt stevensite decays to cobalt orthosilicate (Co_2SiO_4) and zinc stevensite to zinc silicate (Zn_2SiO_4). A third example is an article by Roelofs and Berben [12] regarding the synthesis of organophilic stevensite clay, which evaluated the effect of incorporating low-density polyethylene (LDPE) nanoparticles. The synthesis was produced in an aqueous solution with sodium silicate, urea, and zinc nitrate, with an initial pH of 1.5 (adjusted with nitric acid). The dispersion was heated to 90 °C and when it reached 65-70 °C, a hot solution of acidified dimethyloctadecylamine was added. Subsequently, the solution was left over heating at 90 °C, and stirred for 16-20 h. The results showed that the organophilized stevensite clay was synthesized and that the characteristics obtained, such as low stacking number, facilitate the formation of nanocomposites. The X-ray diffraction (XRD) and transmission electron microscopy (TEM) of the stevensite/LDPE nanocomposites allowed observing the formation of an exfoliated nanocomposite, besides improving the thermal stability of the polymer. Finally, Hindshaw et al. [18] evaluated the fractionation of the lithium (Li) isotope during the formation of clay

minerals. For this, they synthesized magnesium stevensite and saponite using MgCl_2 and lithium chloride (LiCl). Clays were synthesized using two different methods at 20 °C and with a pH of 9.0 to 10.4, adjusted with hydrochloric acid (HCl): 1) PPE flasks with electrolyte buffer for a period of 9 days; and 2) reaction vessel coupled to an autotitrator for a period of 14 days. According to the authors, magnesium-rich saponite and stevensite were synthesized.

Although some authors report the synthesis of stevensite smectite [12, 18, 23, 24], the subject is little studied. For this reason, the objective of the present study was to synthesize a zinc-rich stevensite hydrolyzing urea at low temperature by a practical and simple process that produces clays exhibiting properties equal to those of superior quality to naturally occurring stevensites and synthetic stevensites. In this study, the effect of pH-regulating acids and synthesis methods were evaluated. This knowledge is essential to allow the stevensite clay synthesis process to gain greater industrial use and to be expanded to different high-value-added applications.

MATERIALS AND METHODS

The reagents used as the silicon and zinc source in the synthesis process were, respectively, sodium metasilicate pentahydrate ($\text{Na}_2\text{SiO}_3 \cdot 5\text{H}_2\text{O}$, Nuclear) and zinc nitrate hexahydrate $[\text{Zn}(\text{NO}_3)_2 \cdot 6\text{H}_2\text{O}$, Synth]. Urea $[\text{CO}(\text{NH}_2)_2$, Neon] was used to complete the reaction mixture [15]. Two acids were also used to adjust pH: concentrated nitric acid (HNO_3) and concentrated hydrochloric acid (HCl), one of the paper innovations. An osmosis purified water system was used.

Synthesis of stevensite: the synthesis was based on a simplification of the process described by Hildebrando

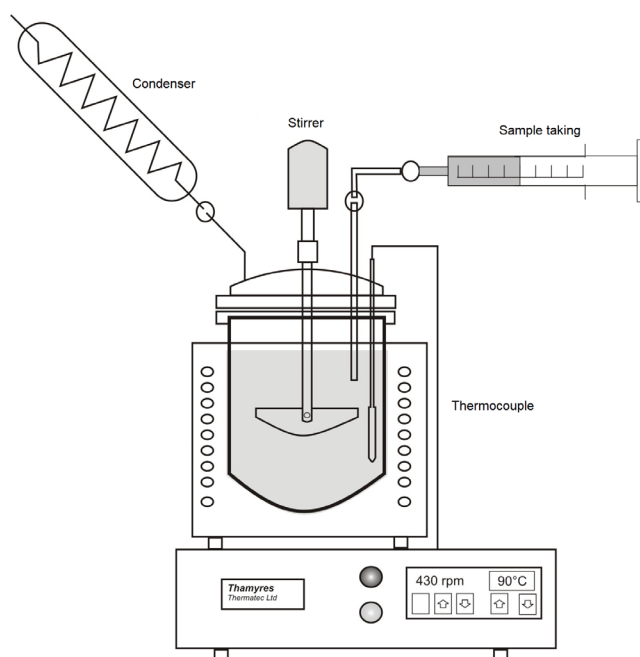


Figure 1: Outline of the dynamic synthesis process.

et al. [15], performed using two processes, static and dynamic with nitric acid (more often used in the literature) and hydrochloric acid. The first solution was prepared by the dilution of 90 g of $\text{Na}_2\text{SiO}_3 \cdot 5\text{H}_2\text{O}$ and 45 g of $\text{CO}(\text{NH}_2)_2$ in 500 mL of water, with a magnetic stirrer, at an initial pH in the range between 1-2, adjusted with nitric acid [15] and hydrochloric acid. Then, 45 g of $\text{Zn}(\text{NO}_3)_2 \cdot 6\text{H}_2\text{O}$ were added and the solutions were finally placed under mechanical stirring for 5 min (25 °C, room temperature) leading to the formation of a rather thick gel. In the static process, the aliquot of the solution obtained was conditioned in a closed glass reaction vessel and placed in an oven at 90 °C without stirring for periods of 24, 48, 72, 168, 192, 216, 240, and 336 h. In the dynamic process, the solution was introduced into the reactor (Fig. 1) at 90 ± 5 °C under constant agitation; at 0.25, 0.5, 1, 2, 3, 4, 24, and 48 h, aliquots of 20 mL of solution were taken. After the synthesis process, the samples were filtered, washed with water, and dried at 90 °C for 24 h. The samples were named according to the pH-regulating acid process (static or dynamic) and the synthesis time. For example: EAN24 - E: stevensite, AN: nitric acid, 24: synthesis time in the static process in hours; EANR24 - E: stevensite, AN: nitric acid, R: dynamic process, 24: synthesis time in hours.

Characterization: the samples were characterized by X-ray fluorescence spectroscopy (XRF), X-ray diffraction (XRD), scanning electron microscopy (SEM), Fourier transform infrared spectroscopy (FTIR), and thermogravimetry and derivative thermogravimetry (TG/DTG). The chemical composition of clay samples was characterized by XRF, using a spectrometer (Zetium, Malvern Panalytical). Loss on ignition (L.O.I.) was carried out at 1020 °C for 2 h. XRD analyses were performed with a diffractometer (X'Pert Pro Mpd, PANalytical) using $\text{CuK}\alpha$ radiation ($\lambda=1.5406$ Å), 40 kV voltage, 30 mA current, scanning between 2θ from 5° to 70°, and scanning speed of 2 °/min. XRD patterns of the samples were obtained before and after exposure of the clay to ethylene glycol vapors. This process aimed to evaluate the possibility of expansion of the clay layers, which could be detected by an increase in the d_{001} peak [15, 25]. Samples were analyzed by FTIR using a spectrometer (Nicolet iS5, Thermo Fisher Sci.), scanning from 4000 to 650 cm^{-1} [26]. The morphology and dimensions of clay particles were evaluated by SEM (Inspect 50, FEI). The samples for the SEM analysis were coated with gold [7]. The thermal analyses (TG/DTG) of the clay were performed in a thermal analyzer (STA449F3A-0715-M,

Netsch) under nitrogen flow, between 20 and 1000 °C with a heating rate of 20 °C/min [27].

RESULTS AND DISCUSSION

X-ray fluorescence (XRF): the chemical composition of synthetic clay (EAN and EAC) described in Table I was obtained from XRF analysis. The main constituent of clays was silicon oxide (EAN: 59.1% and EAC: 61.1%). Aluminum oxide was present (0.1%), probably due to the material in the sample holder; in addition, zinc oxide (25.6-27.8%) was identified as a composition of a trioctahedral zinc smectite corresponding to stevensite. A small percentage of chlorine was observed for the EAC clay (0.8%), indicating the presence of hydrochloric acid in the synthesis. The presence of chlorine may influence the decrease in the percentage of ZnO in EAC clay, due to Cl occupying positions in the octahedral layer instead of Zn. The value of L.O.I. corresponded to the loss in mass resulting from the heat treatment of the sample at 1020 °C. The L.O.I. values were observed not to exceed 12%, indicating a low amount of organic matter in relation to the mineral fraction in the sample. This result agreed with that observed in the infrared analysis [25].

X-ray diffraction: the XRD patterns of the samples prepared by the static and dynamic methods are shown in Figs. 2 and 3, respectively. The clays exhibited similar behavior and characteristics to that of synthetic stevensite clay, suggested by the peaks at $2\theta= 5.8^\circ$ (12.8-15 Å), 19.8° (4.57 Å), and 34.6° (2.61 Å) [7, 15, 28]. The values found were also similar to those of natural stevensite clay, as observed in other studies [29-31]. The refraction at $2\theta=60.6^\circ$ (1.53 Å) observed is typical of trioctahedral smectite clay. In addition, the XRD results revealed the presence of ZnO, corresponding to a peak at 34.6° (2.61 Å), according to the standard crystallography database (JCPDS 36-1451), indicating the formation of synthetic zinc-rich stevensite, and in agreement with XRF and FTIR analyses. A longer synthesis time in the static method contributed to the increase of the crystallinity of the EAN clay with no significant changes observed in the EAC clay, which may be observed by a better definition of the peaks (Fig. 2). The positive effect on the crystallinity may be related to the better stacking of the layers due to the aging, which allowed for a higher ordering of the structure. Moreover, the HCl replacement may have delayed the material crystallization [8]. The characteristic patterns of the stevensite clays produced by the dynamic method with nitric acid (Fig. 3a) and with hydrochloric acid (Fig. 3b) showed that for shorter

Table I - Chemical analysis data (wt%) of stevensite EAN and EAC

Clay	Na_2O	MgO	Al_2O_3	SiO_2	SO_3	Cl	K_2O	CaO	Fe_2O_3	ZnO	L.O.I.
EAN	1.2	-	0.1	59.1	-	-	-	-	-	27.8	11.9
EAC	1.3	-	0.1	61.1	-	0.8	-	-	-	25.6	11.1

L.O.I.: weight loss on ignition at 1020 °C.

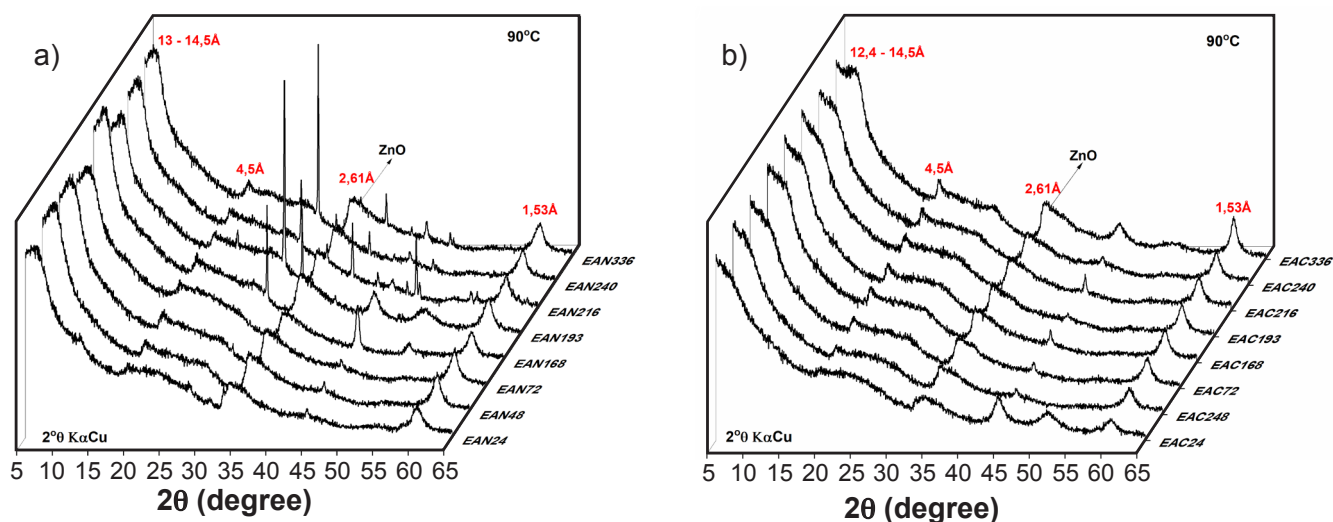


Figure 2: X-ray diffraction curves of clays produced at 90 °C by the static method with: a) nitric acid (EAN); and b) hydrochloric acid (EAC)

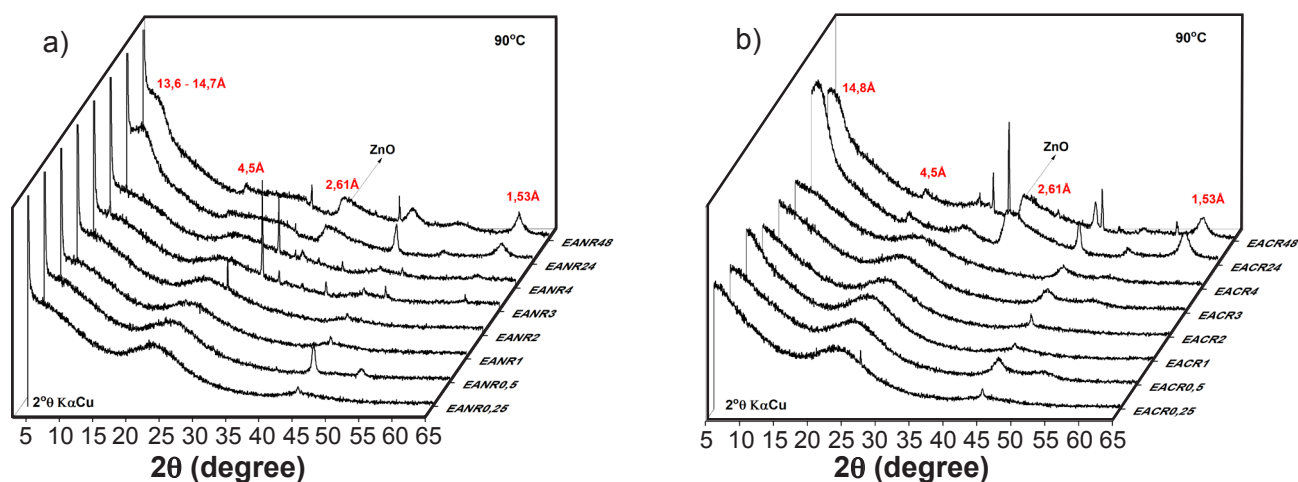


Figure 3: X-ray diffraction curves of clays synthesized at 90±5 °C by the dynamic method with: a) nitric acid (EANR); and b) hydrochloric acid (EACR).

times, a synthesis temperature of 90 °C was not sufficient for the reagents to react and produce the stevensite clay. According to Roelofs and Berben [12], the reaction time is strongly dependent on temperature and pressure, and higher temperatures allow shorter synthesis times.

The X-ray diffraction curves allowed observing that a characteristic pattern of stevensite clay was obtained in both synthesis methods and with both acids used to adjust the pH of the initial solution. However, in the static method experiment, greater practicality, simplicity, and speed in the development of the synthesis were observed; that is, as presented in XRD patterns and confirmed in subsequent techniques, the static method presented characteristics of a zinc stevensite clay at low temperature and pressure, with only 24 h of precipitation compared to other methods in the literature, which took 48 h and even weeks, with complex equipment of high cost [17, 30]. Hence the synthesis process presented showed to be feasible and more economic. Another important fact was obtaining stevensite clay using hydrochloric acid instead of nitric acid (a commonly

used acid in the literature [11, 15]) since hydrochloric acid is easier to commercialize, is less expensive and its production causes less pollution when compared to nitric acid (extremely dangerous and polluting). These and the feasibility of large-scale industrial production are points that affect the development of synthetic clays. Based on the XRD results, samples EAN24, EAN48, EAN72, EAC24, EAC48, EAC72, EANR24, EANR48, EACR24, and EACR48 formed the stevensite clay and showed better crystallinity at a shorter synthesis time were chosen for further analysis.

Ethylene glycol treatment: in order to verify the expandability of synthesized clay, the selected samples were submitted to a saturated vapor of ethylene glycol. Table II shows the basal (001) spacings, d_{001} , for the clays after undergoing ethylene glycol saturation. The samples produced in the static method showed considerable interlamellar expansion after ethylene glycol treatment, a result consistent with that obtained by others [3, 29, 32, 33]. The expansibility of the clays produced by the dynamic method was affected, probably because they presented a morphology with more

aggregated particles, as analyzed by SEM; this possibly meant that they required a longer exposure time to ethylene

Table II - Basal spacing d_{001} of clays saturated in ethylene glycol.

Sample	d_{001} (Å)	d_{001} ethylene glycol (Å)
EAN24	13.2	16.0
EAN48	13.3	16.4
EAN72	14.0	18.0
EAC24	14.4	17.0
EAC48	14.4	16.0
EAC72	14.0	16.0
EANR24	14.0	14.0
EANR48	15.0	16.0
EACR24	15.0	-
EACR48	15.0	15.1

glycol to expand. Sample EACR24 did not show the peak at d_{001} after saturation, which suggested a disruption of the clay layers with the introduction of ethylene glycol.

Infrared spectroscopy (FTIR): in the infrared spectra (Figs. 4 and 5), the bands located at around 3650-3690 and 3350-3370 cm^{-1} were attributed to the OH stretching of the clay, typical of trioctahedral smectites [34]. The band at 1624 cm^{-1} corresponded to the stretching vibrations of the OH group, related to the adsorbed water present in the smectite [3, 33, 35]. The band around 1000-1060 cm^{-1} corresponded to the stretching vibrations of the Si-O-type bonds [3, 34, 35], and the band at 660 cm^{-1} corresponded to the vibration of the Si-O-Zn bond in tetrahedral sheets [33, 35, 36]. Furthermore, it was observed that the band at 1000-1060 cm^{-1} showed a decrease in intensity and became less diffuse with increasing synthesis time, which may indicate strong coordination of the zinc metal ion [33]. It was noted that there were no significant changes in the clay mineral specific bands in the spectra of the clays; however, the appearance of

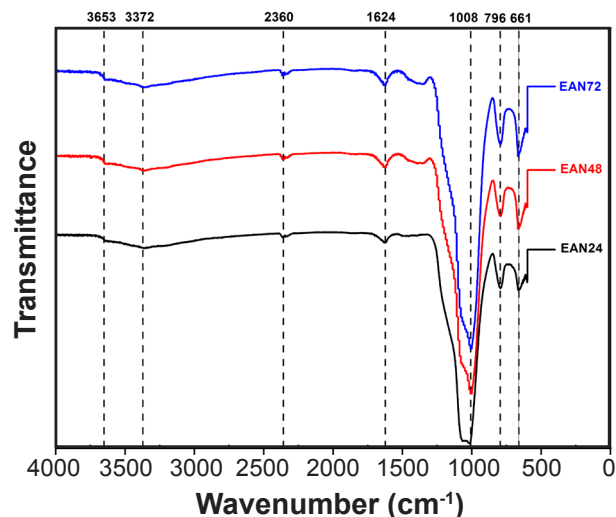
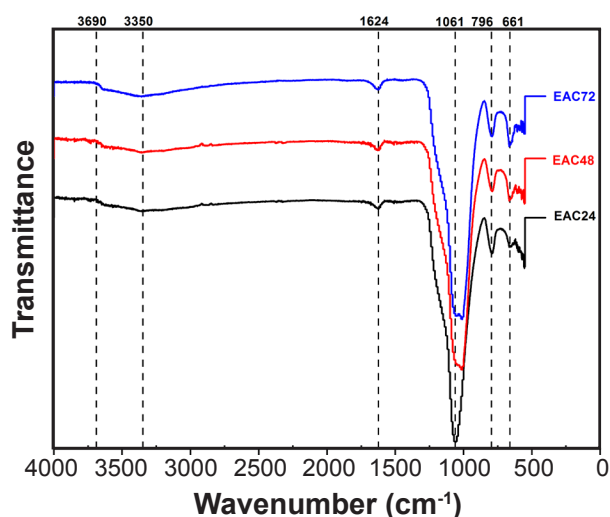


Figure 4: FTIR spectra of clays synthesized by the static method: a) EAN; and b) EAC.

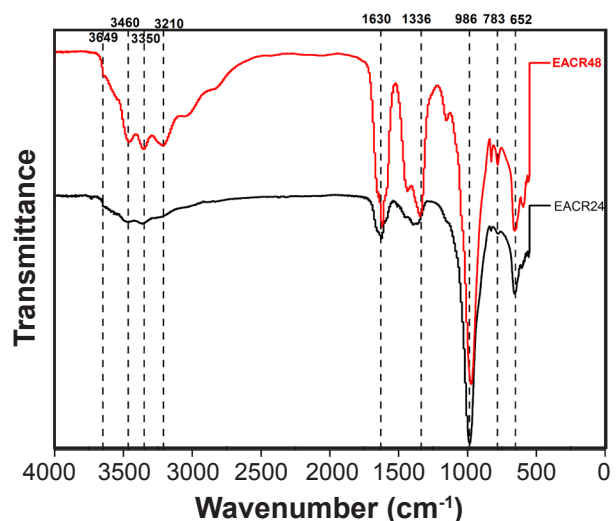
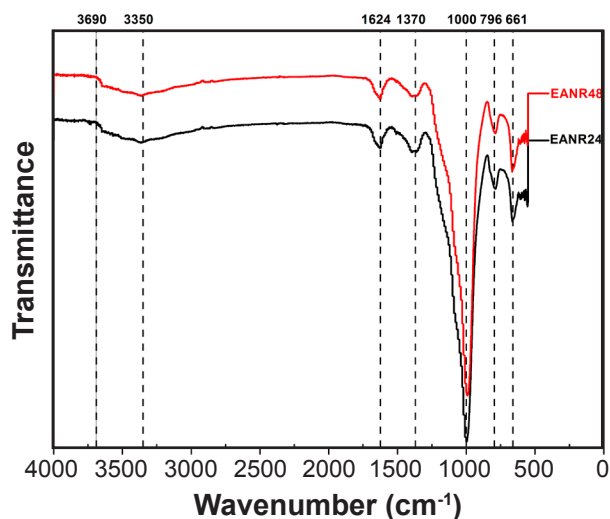


Figure 5: FTIR spectra of the clays synthesized by the dynamic method: a) EANR; and b) EACR.

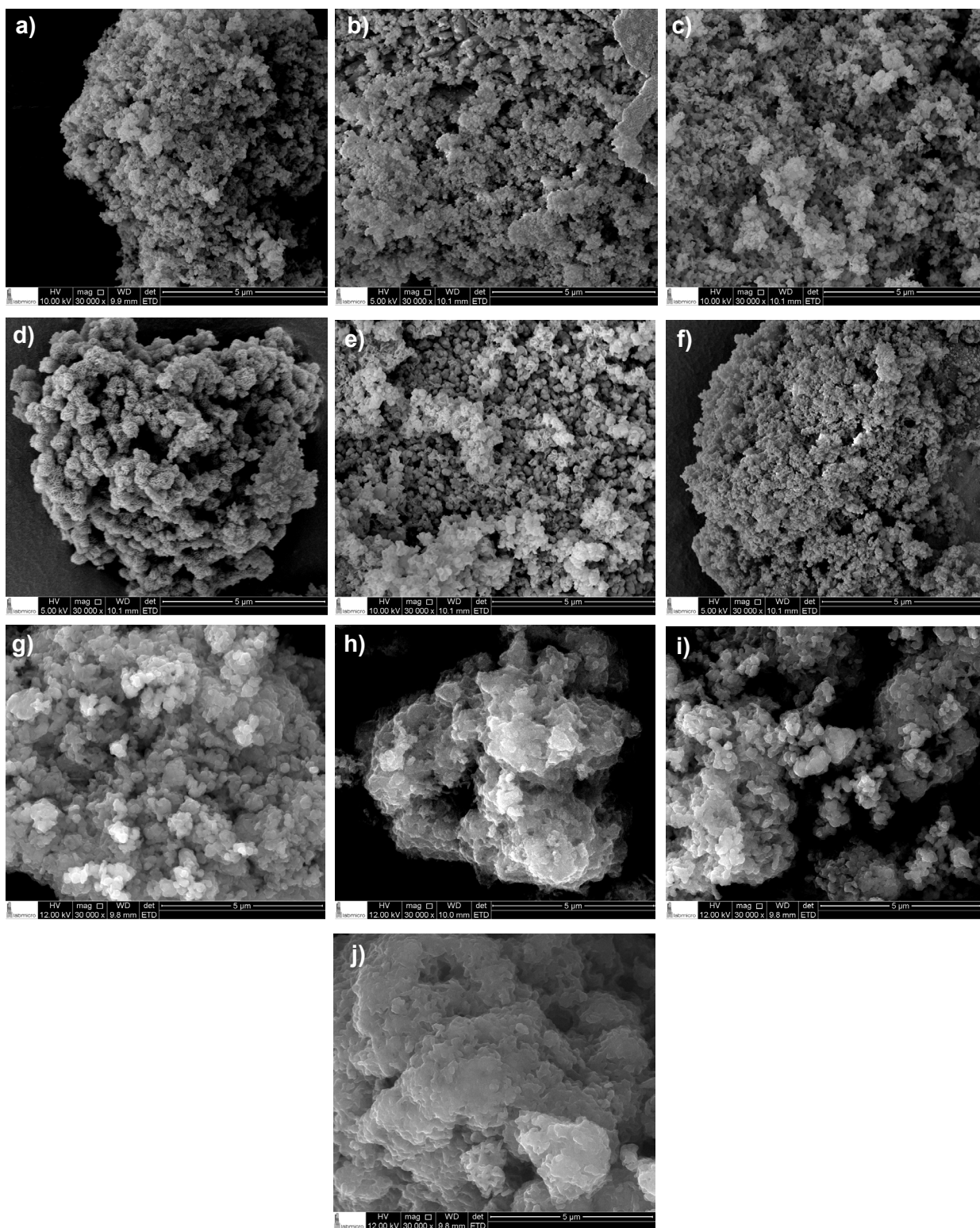


Figure 6: SEM micrographs of the synthesized clays: a) EAN24; b) EAC24; c) EAN48; d) EAC48; e) EAN72; f) EAC72; g) EANR24; h) EACR24; i) EANR48; and j) EACR48

three bands at 3460, 3350, and 3210 cm^{-1} was observed in clays EANR24 and EACR48 (Figs. 5a and 5b, respectively), which was probably due to the presence of adsorbed water molecules [3]. The band at 1336 cm^{-1} was possibly related to the undissolved urea and nitrate reaction products [3, 33].

Scanning electron microscopy (SEM): Fig. 6 shows the SEM images of the clays. From the micrographs, it was possible to observe that the clays had a similar behavior: they appeared to be quite uniform, with regular faces, a characteristic of crystalline materials, and a porous structure

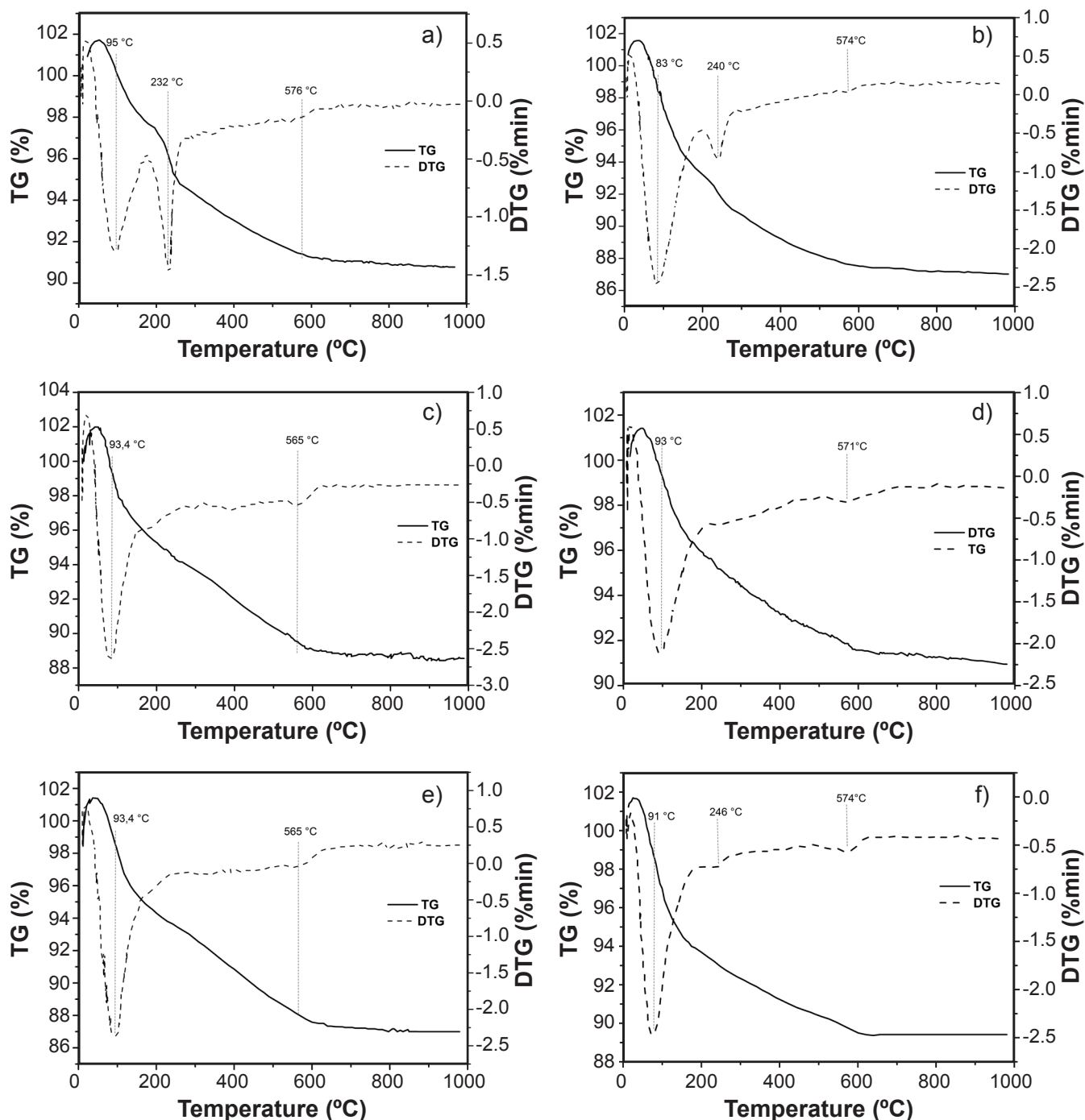


Figure 7: TG and DTG curves of the synthesized clays EAN (a,c,e) and EAC (b,d,f) for 24 h (a,b), 48 h (c,d), and 72 h (e,f) by the static method.

[12]. At the shortest synthesis times, small, regular, and uniform particles with dimensions of the order of nanometers and diameters of approximately 200 nm were observed, which tended to aggregate and coil at the edges, a typical structure of smectite clays [22, 37]. Similar behavior was verified by other authors [7, 15, 38]. As the synthesis time increased, the particle size of the agglomerates decreased (diameter of approximately 100 nm) and the lamellar structure typical of smectites became more visible. This result is important because natural clays generally have diameters greater than

1 μm . The micrographs showed that there were no major changes in the particle morphology of the clays produced with nitric acid and with hydrochloric acid. The use of hydrochloric acid in the synthesis did not cause significant changes in the morphology of the clay, corroborating the results from the XRD analysis and emphasizing the use of HCl as a lower-cost route for producing stevensite.

Thermogravimetry and derivative thermogravimetry (TG/DTG): the thermal stability of the clays was analyzed by TG/DTG (Figs. 7 and 8). The clays showed an intense

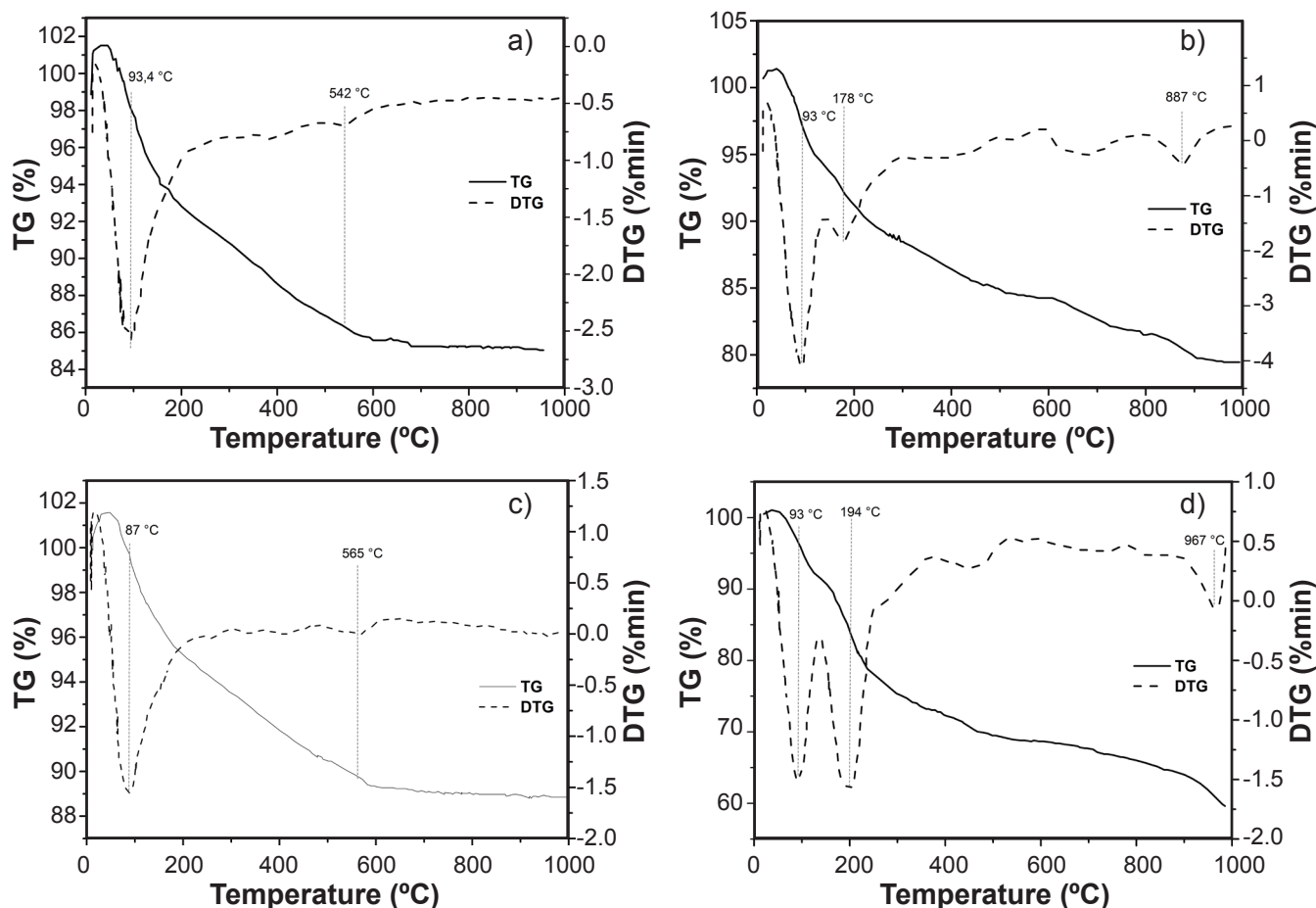


Figure 8: TG and DTG curves of the synthesized clays EANR (a,c) and EACR (b,d) for 24 h (a,b) and 48 h (c,d) by the dynamic method.

peak in the range of $\sim 80\text{--}95$ °C, indicating the loss of adsorbed water from the clay [37], a behavior also observed by Higashi *et al.* [36]. For some clays, the formation of a peak was observed at ~ 210 °C, referring to the loss of water coordinated to interlamellar cations [37]. This peak was more evident in the samples produced with HCl and can probably be related to greater ease for these samples to absorb water. It was observed that some clays also showed a small peak at approximately 540–560 °C, which can be attributed to the dehydroxylation of stevensite [39, 40]. The dehydroxylation temperature depends on the type of intercalary cations (Na^+ , Zn^{2+}) and may vary according to their heterogeneity [36]. In the synthetic clay EACR (Figs. 8b and 8d), a peak was observed at around 890 or 960 °C, which corresponded to phase transformation processes from stevensite into its polymorphs (Zn_2SiO_4) [15, 36, 39–41]. In general, no changes in the thermal behavior of the samples were observed when they were obtained with different acids.

CONCLUSIONS

The present study evaluated two synthetic stevensite clay synthesis processes to make the synthesis process more practical and feasible. The results showed that it was possible to synthesize Zn-stevensite smectite clay at a low

temperature and pressure using both methods. The static process using hydrochloric acid to regulate the pH stood out because it is a simple and economic method (without sophisticated equipment) and because it reduces the time of the synthesis process of zinc stevensite by 50%, compared to the methods established in the literature. The use of hydrochloric acid in the development of the synthesis was essential since it is an acid of easier commercialization for large-scale production compared with nitric acid. The X-ray diffraction patterns suggested that the clays produced are expandable and their morphology is composed of small regular and uniform particles in the order of 100 nm, unlike the natural form that usually presents particles on the order of micrometers. The techniques and characteristics presented in the present study are important for future applications of the new synthetic stevensite.

ACKNOWLEDGMENTS

This work was financially supported by the Coordenação de Aperfeiçoamento de Pessoal de Nível Superior - Brazil (CAPES - Coordination for the Improvement of Higher Education Personnel), and FAPESP (Fundação de Amparo à Pesquisa de São Paulo/the São Paulo Research Foundation), grant number 2019/01231-2. The authors thank the financial

and infrastructural assistance provided by PMT (Department of Metallurgical and Materials Engineering at USP), as well as the Electron Microscopy and Atomic Force Laboratory of the PMT for the SEM facility, LAREX Laboratory for XRD, and the Mackenzie Presbyterian University for the thermal analysis facilities.

REFERENCES

- [1] R. Ishii, N. Teshima, T. Ebina, F. Mizukami, J. Colloid Interface Sci. **348**, 2 (2010) 313.
- [2] R.E. Grim, N. Güven, *Bentonites: geology, mineralogy, properties, uses*, Elsevier, New York (1978).
- [3] F. Franco, M. Pozo, J.A. Cecilia, M. Benítez-Guerrero, M. Lorente, Appl. Clay Sci. **120** (2016) 70.
- [4] H. Li, Y. Li, L. Xiang, Q. Huang, J. Qiu, H. Zhang, M.V. Sivaiah, F. Baron, J. Barrault, S. Petit, S. Valange, J. Hazard. Mater. **287** (2015) 32.
- [5] A.A.M. Lopez, M.A.V. Rodriguez, V.E. Reyes-Cruz, Chem. Eng. Trans. **41** (2014) 55.
- [6] P.G. Lins, T.S. Valera, N.R. Demarquette, Mater. Sci. Forum **727-728** (2012) 929.
- [7] C.S. Pascua, M. Ohnuma, Y. Matsushita, K. Tamura, H. Yamada, J. Cuadros, J. Ye, Appl. Clay Sci. **48**, 1-2 (2010) 55.
- [8] J.T. Klopogge, S. Komarneni, J.E. Amonette, Clays Clay Miner. **47**, 5 (1999) 529.
- [9] D. Zhang, C.H. Zhou, C.X. Lin, D.S. Tong, W.H. Yu, Appl. Clay Sci. **50** (2010) 1.
- [10] Y. Kurokawa, H. Yasuda, A. Oya, J. Mater. Sci. Lett. **15** (1996) 1481.
- [11] A. Pozsgay, L. Papp, T. Fráter, B. Pukánszky, in "Adsorption and nanostructure", I. Dékány (Ed.), Springer, Berlin (2001) 120.
- [12] J.C.A.A. Roelofs, P.H. Berben, Appl. Clay Sci. **33**, 1 (2006) 13.
- [13] H. Kimura, A. Nakashima, S. Takahashi, A. Tsuchida, K. Kurosaka, Appl. Clay Sci. **114** (2015) 120.
- [14] K.A. Carrado, A. Decarreau, S. Petit, F. Bergaya, G. Lagaly, in "Dev. Clay Sci." **1** (2006) 115.
- [15] E.A. Hildebrando, M.G. Silva-Valenzuela, R.F. Neves, F.R. Valenzuela-Diaz, Cerâmica **60**, 354 (2014) 273.
- [16] R.S. Hindshaw, R. Tosca, N.J. Tosca, E.T. Tipper, Earth Planet. Sci. Lett. **531** (2020) 115980.
- [17] S. Guggenheim, in "Magnesian clays charact. orig. appl.", 2nd ed., M. Pozo, E. Galán (Eds.), AIPEA, Digilabs Pub., Bari (2016).
- [18] R.S. Hindshaw, R. Tosca, T.L. Goût, I. Farnan, N.J. Tosca, E.T. Tipper, Geochim. Cosmochim. Acta **250** (2019) 219.
- [19] H. Moussout, H. Ahlafi, M. Aazza, R. Chfaira, C. Mounir, Heliyon **6**, 3 (2020).
- [20] N. Takahashi, M. Tanaka, T. Satoh, T. Endo, M. Shimada, Microporous Mater. **9** (1997) 35.
- [21] D.E. González-Santamaría, E. López, A. Ruiz, R. Fernández, A. Ortega, J. Cuevas, Clay Miner. **52**, 3 (2017) 341.
- [22] A. Benhammou, A. Yaacoubi, L. Nibou, B. Tanouti, J. Colloid Interface Sci. **282**, 2 (2005) 320.
- [23] A. Decarreau, Geochim. Cosmochim. Acta **49**, 7 (1985) 1537.
- [24] A.A. Khassin, T.M. Yurieva, G.N. Kustova, L.M. Plyasova, T.A. Krieger, I.Sh. Itenberg, M.P. Demeshkina, T.V. Larina, V.F. Anufrienko, V.N. Parmon, Mater. Res. Innov. **4**, 4 (2001) 251.
- [25] G.M. Faust, T. George, J.C. Hathaway, Am. Mineral. **44** (1959) 342.
- [26] G.E. Christidis, E. Koutsopoulou, Bull. Geol. Soc. Greece **47**, 1 (2016) 366.
- [27] A. Benhammou, A. Yaacoubi, L. Nibou, J.P. Bonnet, B. Tanouti, Environ. Technol. **32**, 4 (2011) 363.
- [28] M. Sychev, R. Prihod'ko, A. Koryabkina, E.J.M. Hensen, J.A.R. Van Veen, R.A. Van Santen, Stud. Surf. Sci. Catal. **143** (2000) 257.
- [29] R. Fernández, A.I. Ruiz, C. García-Delgado, D.E. González-Santamaría, R. Antón-Herrero, F. Yunta, C. Poyo, A. Hernández, E. Eymar, J. Cuevas, Sci. Total Environ. **645** (2018) 146.
- [30] S. Azarkan, A. Peña, K. Draoui, C.I. Sainz-Díaz, Appl. Clay Sci. **123** (2016) 37.
- [31] R. Antón-Herrero, C. García-Delgado, M. Alonso-Izquierdo, G. García-Rodríguez, J. Cuevas, E. Eymar, Appl. Clay Sci. **160** (2018) 162.
- [32] G.W. Brindley, D.L. Bish, H.-M. Wan, Mineral. Mag. **41**, 320 (1977) 443.
- [33] J.T. Klopogge, M. Hammond, L. Hickey, R.L. Frost, J. Mater. Sci. Lett. **21** (2002) 931.
- [34] J. Madejová, Vib. Spectrosc. **31** (2003) 1.
- [35] S. Yokoyama, K. Tamura, T. Hatta, S. Nemoto, Y. Watanabe, H. Yamada, Clay Sci. **13** (2006) 75.
- [36] S. Higashi, K. Miki, S. Komarneni, Clays Clay Miner. **50**, 3 (2002) 299.
- [37] P. Souza Santos, *Ciência e tecnologia de argilas*, 2nd ed., Edgard Blücher, S. Paulo (1989).
- [38] R. Srivastava, S. Fujita, M. Arai, Appl. Clay Sci. **43**, 1 (2009) 1.
- [39] G.T. Faust, K.J. Murata, Am. Mineral. **38** (1953) 973.
- [40] R. Bejjajoui, A. Benhammou, L. Nibou, B. Tanouti, J.P. Bonnet, A. Yaacoubi, A. Ammar, Appl. Clay Sci. **49**, 3 (2010) 336.
- [41] S. Petit, D. Righi, A. Decarreau, Clays Clay Miner. **56**, 6 (2008) 645.

(Rec. 04/10/2021, Rev. 13/01/2022, 21/04/2022, Ac. 27/04/2022)